Atmosphere-ocean ozone exchange: A global modeling study of biogeochemical, atmospheric, and waterside turbulence dependencies

L. Ganzeveld,[1,2] D. Helmig,[3] C. W. Fairall,[4] J. Hare,[5] and A. Pozzer[2,6]

Received 9 July 2008; revised 12 June 2009; accepted 17 July 2009; published 7 November 2009.

[1] The significance of the removal of tropospheric ozone by the oceans, covering ~2/3 of the Earth's surface, has only been addressed in a few studies involving water tank, aircraft, and tower flux measurements. On the basis of results from these few observations of the ozone dry deposition velocity (V_{dO3}), atmospheric chemistry models generally apply an empirical, constant ocean uptake rate of 0.05 cm s^{-1}. This value is substantially smaller than the atmospheric turbulent transport velocity for ozone. On the other hand, the uptake is higher than expected from the solubility of ozone in clean water alone, suggesting that there is an enhancement in oceanic ozone uptake, e.g., through a chemical destruction mechanism. We present an evaluation of a global-scale analysis with a new mechanistic representation of atmosphere-ocean ozone exchange. The applied atmosphere chemistry-climate model includes not only atmospheric but also waterside turbulence and the role of waterside chemical loss processes as a function of oceanic biogeochemistry. The simulations suggest a larger role of biogeochemistry in tropical and subtropical ozone oceanic uptake with a relative small temporal variability, whereas in midlatitude and high-latitude regions, highly variable ozone uptake rates are expected because of the stronger influence of waterside turbulence. Despite a relatively large range in the explicitly calculated ocean uptake rate, there is a surprisingly small sensitivity of simulated Marine Boundary Layer ozone concentrations compared to the sensitivity for the commonly applied constant ocean uptake approach. This small sensitivity points at compensating effects through inclusion of the process-based ocean uptake mechanisms to consider variability in oceanic O_3 deposition consistent with that in atmospheric and oceanic physical, chemical, and biological processes.

Citation: Ganzeveld, L., D. Helmig, C. W. Fairall, J. Hare, and A. Pozzer (2009), Atmosphere-ocean ozone exchange: A global modeling study of biogeochemical, atmospheric, and waterside turbulence dependencies, *Global Biogeochem. Cycles*, *23*, GB4021, doi:10.1029/2008GB003301.

1. Introduction

[2] The removal of trace gases and aerosols at the Earth's surface by dry deposition provides an important sink for many atmospheric trace gases such as ozone. The estimated global annual sink of this photo-oxidant, air pollutant, and greenhouse gas through dry deposition of 600–1000 Tg O_3 yr^{-1} is comparable to the tropospheric source of ozone through stratosphere-troposphere exchange. These estimates are based on simulations with global atmospheric chemistry models that incorporate our best understanding of transport processes, photochemical formation in the troposphere and surface deposition [e.g., *Ganzeveld and Lelieveld*, 1995; *Brasseur et al.*, 1998; *Lelieveld and Dentener*, 2000; *Bey et al.*, 2001; *von Kuhlmann et al.*, 2003]. Application of these models is not limited to the assessment of the global sources and sinks of species such as ozone. Such models are applied to simulate scenarios of the impacts of future environmental changes, such as urbanization, land use change, and the anticipated rise in global temperatures on the atmospheric ozone budget and climate. Substantial efforts are put into improvements of the so-called online models, such as the chemistry-climate model ECHAM4 [*Ganzeveld et al.*, 2002] and ECHAM5/MESSy [*Jöckel et al.*, 2006], which allow more explicit studies of the feedbacks between

[1]Department of Environmental Sciences, Wageningen University and Research Centre, Wageningen, Netherlands.
[2]Department of Atmospheric Chemistry, Max-Plank Institute for Chemistry, Mainz, Germany.
[3]Institute of Arctic and Alpine Research, University of Colorado, Boulder, Colorado, USA.
[4]Earth Systems Research Laboratory, National Oceanic and Atmospheric Administration, Boulder, Colorado, USA.
[5]Cooperative Institute for Research in Environmental Sciences, University of Colorado, Boulder, Colorado, USA.
[6]Now at the Cyprus Institute, Energy, Environment and Water Research Center, Nicosia, Cyprus.

0886-6236/09/2008GB003301$12.00

Table 1. Literature With Ozone Flux Measurements Over Ocean and Lakes

Location	Technique	Deposition Velocity (cm s^{-1})	Reference
Sea water	Box enclosure decay	0.03–0.06	*Aldaz* [1969]
Fresh water	Box enclosure decay	0.1	
Sea water	Profile method	0.08–0.15	*Tiefenau and Fabian* [1972][a]
Sea water	Wind tunnel	0.04	*Garland and Penkett* [1976]
Sea water	Laboratory	0.025–0.09	*Galbally and Roy* [1980]
Fresh water	Laboratory	0.015–0.1	
Lake water	Tower eddy correlation	0.01	*Wesely et al.* [1981]
Gulf of Mexico, North Pacific	Aircraft eddy correlation	0.056	*Lenschow et al.* [1982]
Sea water, off Southern California	Aircraft eddy correlation	0.02	*Kawa and Pearson* [1989]
Sea water and saline solutions	Static chamber technique	0.006–0.014	*McKay et al.* [1992]
South Atlantic	Budget	0.03	*Heikes et al.* [1996]
Sea water	Literature review	0.01–0.05	*Wesely and Hicks* [2000]
Fresh water		0.01	
Coastal region North Sea	Tower eddy correlation	0.11	*Gallagher et al.* [2001]

[a]Referenced by *McKay et al.* [1992].

chemistry and climate. These online models include to some extent the role of changing greenhouse gas and aerosol burdens on the radiative forcing and hydrological cycle.

[3] Some of these current atmospheric chemistry models contain rather explicit representations of dry deposition including turbulent transport and diffusion to the surface and active removal by surface substrates such as vegetation, soils and water. However, a major limitation with respect to the representation of dry deposition in large-scale models is the limited number of observations that have provided quantification of dry deposition over various surface cover types and identification of the controlling mechanisms. The latter is essential to develop more mechanistic representations in atmospheric chemistry or Earth system models in order to improve their predictive capacity. One of the surfaces for which there is only a small selection of observations available are the world's oceans. Ozone deposition into the oceans represents a significant loss from the atmosphere with current best estimates, based on chemistry-transport model analyses, indicating that oceanic ozone deposition accounts for about one third of the global annual ozone deposition of 600–1000 Tg O_3 yr^{-1} [e.g., *Ganzeveld and Lelieveld*, 1995; *Ganzeveld et al.*, 2002; *von Kuhlmann et al.*, 2003].

[4] In this paper we discuss, in section 2, the currently available observations of ozone dry deposition not only in terms of the magnitude and variability but also in terms of mechanisms that drive ozone uptake by the world's oceans. From this information a parameterized description of oceanic ozone deposition was applied to assess the sensitivity of atmospheric O_3 to oceanic deposition. The outcome of this sensitivity analysis motivated the here presented more detailed study on oceanic O_3 deposition for which we applied a more mechanistic model of oceanic dry deposition including atmospheric and waterside turbulence and chemical destruction (section 3). In section 4 we describe the compilation of global oceanic concentrations of iodide, one of the species involved in the chemical destruction of ozone, and present an evaluation of this new mechanistic representation of oceanic O_3 dry deposition in section 5. In addition, we present in section 6 an assessment of the role of oceanic ozone dry deposition for the global ozone deposition budget, boundary layer concentrations, and transport, followed by conclusions and outlook.

2. Oceanic Ozone Dry Deposition: Mechanism

[5] The ozone dry deposition flux is generally calculated in atmospheric chemistry models as the product of the atmospheric surface layer concentration and the dry deposition velocity (V_d), which reflects the efficiency of removal at the Earth's surface. A number of these atmospheric chemistry models nowadays apply dry deposition algorithms to explicitly calculate V_d as the reciprocal of three serial resistances: $V_d = (R_a + R_b + R_s)^{-1}$ [*Wesely and Hicks*, 2000]. R_a is the aerodynamic resistance reflecting the turbulent transport to the ocean surface, R_b is the quasi-laminar boundary layer resistance, which describes the quasi-laminar transport through a thin layer of air in contact with the ocean surface, and R_s is the oceanic surface resistance. R_s reflects the efficiency of transfer and destruction of ozone by physical, chemical and biological processes along the pathway ending at the ultimate site of ozone destruction, i.e., where $[O_3]_{ocean}$ equals zero (this is why $[O_3]_{ocean}$ cancels out of the calculation of the flux from the O_3 gradient between the atmospheric and oceanic surface layer). More details on the theory and actual calculation of the oceanic O_3 dry deposition velocity are provided by *Fairall et al.* [2007].

[6] A summary of reported ozone dry deposition velocities over ocean and fresh water including the applied measurement techniques is given in Table 1. Earlier methods relied on enclosure systems, where the decay of ozone is studied within a box that is placed over water. Compared to enclosure studies, ambient level measurements are advantageous because they minimize environmental disturbances and allow investigation of surface-atmosphere gas exchange under a variety of conditions. Flux measurements by the eddy covariance measurement (ECM) technique have become the preferred technique because of its sensitivity and capability to facilitate continuous flux measurements that are representative for large footprint areas. However,

only a few ozone ocean flux studies have relied on this approach by application of ECM from fixed tower platforms [*Gallagher et al.*, 2001], or by turbulent aircraft measurements [*Lenschow et al.*, 1982; *Kawa and Pearson*, 1989]. Actually, the analysis presented here has been conducted within an research project that includes the deployment of an eddy covariance ozone flux measurement system on board the NOAA ship *Ronald H. Brown*. These observations are under analysis and will be presented in more detail in a forthcoming publication [*Bariteau et al.*, 2009].

[7] Obviously, a large range of deposition velocities is reported with values ranging from $V_{dO3} \sim 0.01$ to 0.15 cm s^{-1} for ocean water, and $0.01 - 0.10$ cm s^{-1} for fresh water, which is much smaller than continental ozone deposition velocities. For example, the observed daytime tropical forest V_{dO3} shows maximum values up to 2 cm s^{-1} [e.g., *Fan et al.*, 1990] due to efficient uptake of ozone by the leaf stomata. Oceanic O_3 deposition velocities are significantly smaller compared to the atmospheric transport velocity (reciprocal of aerodynamic resistance) suggesting that there is a significant resistance against surface uptake. On the other hand, the average surface uptake rate, inferred from the observations, is substantially faster than expected from the ozone water solubility alone ($\sim$ factor 40) suggesting that there is an enhancement, i.e., through chemical destruction [*Schwartz*, 1992], in the water. For example, it has previously been postulated that ozone ocean deposition might be accelerated due to its reaction with iodide (I^-) [*Garland et al.*, 1980] although these studies found that those reactions cannot explain more than 20% of the enhancement. A later study by *Chang et al.* [2004], who combined data from newer observations and new models of oceanic trace gas exchange, indicated that the iodide-ozone reaction could explain most of the enhanced ozone removal for 293K, low wind speed conditions, and observed iodide concentrations between 20 and 400×10^{-9} M. In addition, *Chang et al.* [2004] also included estimates for the reactions of ozone with dimethyl sulfide (DMS) and alkenes. This analysis indicated that the potential maximum enhancement by the DMS-O_3 reaction is about half the iodide enhancement whereas reactions between alkenes and O_3 were deemed too slow to increase ozone removal. The analysis by *Chang et al.* [2004] leaves unanswered the question how to account for observed ozone uptake rates under conditions of medium to high wind speeds, temperatures substantially different from 293K, and the global range in I^- and DMS concentrations.

[8] Several researchers have noted that the reaction and loss rates of ozone to ocean surface water is expected to be related to the amount of algal biomass and available dissolved organic compounds [*Wesely et al.*, 1981; *Schwartz*, 1992; *Wesely and Hicks*, 2000; *Clifford et al.*, 2008]. *Schwartz* [1992] stated that the penetration depth of ozone into the ocean is only a few μm, suggesting that any chemical enhancement could be controlled by chemical interactions most likely occurring in the microlayer present at the oceanic surface. *McKay et al.* [1992] published a detailed experimental investigation (using a static chamber technique) of the dependence of ozone deposition on water composition. These researchers found a strong correlation between ozone deposition and dissolved surfactant concentrations and inferred a seasonally varying ozone deposition from observed annual variations of surfactants in the samples that were collected off the coast of the United Kingdom. These authors estimated that ozone fluxes may vary seasonally by at least a factor of two. Furthermore, stirring of water resulted in a significant increase of the ozone uptake rate which suggests that near-surface mixing causes an increase of the ozone deposition rate. More recently, a laboratory study by *Clifford et al.* [2008] provided more direct experimental evidence about the role of dissolved organic compounds, including chlorophyll, in removal of ozone by water surfaces.

[9] These considerations underline the need to more carefully study the fluxes of ozone and their dependency on ocean water properties and conditions. A plethora of previous research has demonstrated the importance of these properties on ocean-atmosphere fluxes of other important gases, such as CO_2 and DMS [e.g., *Matrai et al.*, 2006]. Likewise to CO_2, significant differences in O_3 uptake are expected as a function of biological ocean properties. In particular, the effect of the significant spatial and temporal variations of algal biomass and dissolved organic matter in ocean surface water [*Antoine et al.*, 1996; *Peltzer and Hayward*, 1996; *Hansell and Carlson*, 2001] on ozone fluxes is of great interest.

[10] Besides questions concerning the oceanic sink of tropospheric ozone there is also speculation that reactions between ozone and dissolved organic carbon (DOC) at the surface water/atmosphere result in the release of volatile organic compounds (VOC) from ocean water [*Riemer et al.*, 2000] and that these VOC are subsequently released into the atmosphere where they are involved in atmospheric chemical transformations. In particular, *n*-aldehydes, e.g., octanal, nonanal, and decanal have been shown to be formed from the oxidation of unsaturated fatty acids which are derived from decomposing phytoplankton [e.g., *Kieber et al.*, 1997]. Furthermore, several ambient measurement campaigns have illustrated elevated atmospheric aldehyde levels in coastal regions and over the oceans [*Greenberg and Zimmerman*, 1984; *Yokouchi et al.*, 1990; *Ciccioli et al.*, 1993; *Helmig et al.*, 1996]. These observations imply a possible feedback mechanism where atmospheric ozone is deposited to the surface of oceans/lakes and could act as an oxidant of dissolved organic matter resulting in the formation and atmospheric release of VOC's which in turn are involved in atmospheric photochemistry.

3. Global Oceanic Ozone Dry Deposition

[11] In current atmospheric chemistry models, either constant values or explicitly resolved oceanic ozone dry deposition velocities are applied; these values commonly are on the order of 0.05 cm s^{-1} [*Ganzeveld and Lelieveld*, 1995]. Current models that include an explicit representation of the dry deposition process [e.g., *Ganzeveld et al.*, 1998] only consider the variability in oceanic dry deposition velocities due to atmospheric turbulence and diffusion. The ocean surface uptake process does not include any spatial and temporal dependencies on ocean biological, chemical and

physical properties. Thus a global constant water surface uptake resistance is applied.

[12] A strong motivation for the analysis presented here has been a previously conducted sensitivity study (L. Ganzeveld and R. von Kuhlmann, unpublished results, 2004) with the off-line chemistry tracer transport model MATCH-MPIC [*von Kuhlmann et al.*, 2003], where we applied a range in global constant ocean uptake resistances such that we simulated ozone deposition velocities (V_{dO3}) resembling the reported observed range in oceanic V_{dO3}. The sensitivity analysis indicated that imposing the lower estimate of V_{dO3} = 0.01 cm s^{-1} (compared to the standard $V_{dO3} \sim 0.05$ cm s^{-1}, reflecting the default selected constant ocean uptake resistance of 2000 s m^{-1} of the MATCH-MPIC dry deposition scheme) resulted in an substantial increase of simulated surface layer ozone concentrations. The ozone increase was especially large in high-latitude regions over the oceans. The analysis showed relative differences in surface ozone of up to 60%, and as large as 25% at an altitude of 2.5 km, indicating that this sensitivity of ozone concentrations to ocean dry deposition is not limited to the Marine Boundary Layer (MBL).

[13] Quantitatively similar findings were reported by *Shon and Kim* [2002]. Using the low estimate of V_{dO3} = 0.013 cm s^{-1}, these authors found that deposition to the sea surface accounted for 17% of the diurnal MBL ozone loss. Larger losses were calculated using values in the middle to upper range of the previously reported ozone deposition rates (see Table 1). Both our modeled estimate and this literature estimate demonstrate the potential large error in atmospheric chemistry models caused by the inaccurate description of ozone deposition to the sea surface.

[14] Recent research on ocean – atmosphere energy and gas exchange processes, mostly focusing on CO_2 exchange, has resulted in improved models (such as the NOAA/COARE gas transfer model [*Hare et al.*, 2004]) that describe the dependencies of atmosphere-ocean trace gas exchange on a variety of physical mechanisms beyond wind speed alone. This model has recently been extended by considering the role of chemical destruction in the ocean for the exchange of reactive trace gases, such as ozone. It calculates the flux using the bulk atmospheric ozone concentrations accounting for molecular diffusive transfer in both fluids using trace gas specific *Schmidt* numbers in water and air and surface-renewal-type theory to match molecular and turbulent sublayers [*Fairall et al.*, 2000, 2007]. The model also considers the enhancement of exchange at higher wind speeds via whitecap generated bubbles. This enhancement is expected to be relevant to CO_2 exchange, but not for ozone because of the much smaller penetration depth of ozone into seawater, which is on the order of a few μm. The main difference compared to the commonly applied calculation of V_{dO3} over the oceans using a global constant R_s of 2000 s m^{-1} is the explicit consideration of the role of waterside molecular diffusion and turbulence, solubility and reactivity in R_s. Here we present a model analysis based on experiments conducted with a chemistry-climate model including an implementation of the *Fairall et al.* [2007] scheme. The simulations reflect a number of 1-year integrations with the Modular Earth Submodel System (MESSy, version 1) [*Jöckel et al.*, 2006] coupled to the climate model ECHAM5 [*Roeckner et al.*, 2003], allowing for a 1-month model spin-up, using a T42 model resolution ($\sim$2.8°) with 19 layers in the vertical (up to about 10 hPa with $\sim$3–4 layers representing the MBL). These short integrations do not allow assessment of the impact of climate variability on the simulated ozone exchange and atmospheric burden. Instead, the presented analysis aimed at demonstrating the sensitivity of ozone to a more mechanistic representation of oceanic ozone uptake rather than providing a quantitative assessment of oceanic ozone deposition. The climate model was constrained with monthly mean Sea Surface Temperatures (SST) based on a climatology reflecting the period 1979–2001 (AMIP II) [*Taylor et al.*, 2000]. The simulations reflect atmospheric chemistry processes similar as the ones considered for the previously described extensive evaluation of ECHAM5/MESSy [*Jöckel et al.*, 2006], including the gas-phase chemistry module MECCA [*Sander et al.*, 2005], and scavenging and convective tracer transport [*Tost et al.*, 2006]. The technological, agricultural and biomass burning emissions were taken from the EDGARv3.2 fast-track update of the emissions for the year 2000 [*Olivier et al.*, 2005; *van Aardenne et al.*, 2005], whereas dry deposition and biogenic emissions of, i.e., DMS, NO, and isoprene were calculated online [*Ganzeveld et al.*, 2002]. The O_3 dry deposition calculations used ECHAM5s meteorological parameters including surface temperature, humidity, wind speed, and sea ice cover. In addition, the calculations used derived monthly I^- and DMS, and constant alkene oceanic surface water concentrations. The O_3-I^- reaction rate was calculated according to *Magi et al.* [1997] from the SST whereas constant O_3-DMS, O_3-C_2H_4 and O_3-C_3H_6 reaction rates of 6.7 $\times$ 10^8, 1.8 $\times$ 10^5 and 8.0 $\times$ 10^5 M^{-1} s^{-1}, respectively, were applied [*Gershenzon et al.*, 2001; *Dowideit and von Sonntag*, 1998; *Chang et al.*, 2004, Table 1]. The Henry law coefficient for O_3 was corrected for temperature ($H_{O3\text{-}T}$) using an H_0 (H_{O3} for 298K) and enthalpy of 9.4 $\times$ 10^{-3} M atm^{-1} and 2400K, respectively [*Seinfeld*, 1986; *Sander*, 1999]. The salinity has a low impact ($\sim$0.1%) on the solubility of ozone and is, consequently, not included.

[15] The role of waterside diffusion and turbulence, solubility and chemical destruction on the global oceanic O_3 dry deposition was investigated as a function of oceanic biogeochemical properties. This assessment also included the deposition of O_3 to some large freshwater lakes. Since freshwater is expected to exhibit a distinctly different role of biogeochemistry compared to the ocean, a number of large lakes which are explicitly resolved for the selected model resolution were also included in this analysis. However, for simplicity hereafter both systems are referred to as "oceanic" processes. We assessed the role of the chemical enhancement for global ozone oceanic uptake by compiling a global distribution of oceanic iodide concentrations, complemented by the global DMS oceanic concentration fields which are used to calculate online the oceanic DMS emissions in ECHAM5/MESSy. DMS concentrations fields were based on the global inventory by *Kettle and Andreae* [2000]. The relative small role of alkenes in ozone reactive

uptake was considered by applying global annual mean concentrations similar to those applied by *Chang et al.* [2004], i.e., 0.5 nM ethene and 0.2 nM propene. We also considered including the role of isoprene in oceanic O_3 uptake. For typical oceanic isoprene concentrations of 50 pM (according to *Broadgate et al.* [1997]) and an aqueous-phase O_3-isoprene reaction of 4×10^5 M^{-1} s^{-1} (according to *Pedersen and Sehested* [2001]), the O_3-isoprene reactivity is at least 4–5 orders of magnitude smaller compared to the O_3-I^- reactivity. Based on this result we subsequently ignored the role of isoprene in oceanic O_3 uptake. We also ignored the role of sea-salt reactions. These are known to be important for ozone depletion in the marine boundary layer [e.g., *Saiz-Lopez et al.*, 2008] but are not expected to be relevant for oceanic O_3 uptake at the high pH of seawater (Roland von Glasow, School of Environmental Sciences, University of East Anglia, Norwich, United Kingdom, personal communications, 2006).

[16] The main objective of our experiment was to assess the role of first-order destruction rates of ozone with I^-, DMS, C_2H_4 and C_3H_6 in the oceanic surface layer in global oceanic ozone deposition and the implications for the atmospheric burden of ozone. Another question is if and where additional reactions of ozone, for instance by the surfactant layer as postulated by *Schwartz* [1992] and *McKay et al.* [1992], might be required to account for observed uptake rates. Before showing an evaluation of the modeled V_{dO3}, global-scale oceanic ozone deposition and the impact on atmospheric ozone budget in section 5, we first present in section 4 the compilation of the global oceanic iodide fields. For a more detailed discussion on the global oceanic DMS concentrations we refer to *Kettle and Andreae* [2000].

4. Ocean Biogeochemistry: Iodide Concentrations

[17] Iodide (I^-) together with iodate (IO_3^-) make up the bulk of dissolved iodine in seawater, with the remainder being negligible contributions from any organically bound iodine fraction in oxic ocean waters. The total average concentration of dissolved iodine is $\sim$ 0.45 mM [*Truesdale et al.*, 2000]. The oceanic distribution of iodine is regulated by the uptake of dissolved iodine in surface waters into biological material, and its subsequent regeneration at depth from sinking and decomposing organic matter [*Campos et al.*, 1999]. The iodide is produced in surface waters by the reduction of IO_3^-, e.g., through uptake of the IO_3^- by phytoplankton, resulting in the formation of reduced iodine. In turn the chemical oxidation of I^- to IO_3^- is extremely slow for oceanic conditions resulting in a I^- lifetime of years. However, modeling analyses suggest an additional biologically catalyzed oxidation route resulting in a much shorter I^- lifetime compared to that solely based on chemical oxidation [*Campos et al.*, 1999]. *Campos et al.* [1996] proposed that I^- production is directly related to the primary oceanic production via a simple conversion factor. However, an analysis of I^- concentrations along transects in the South Atlantic indicated that this relationship, which previously had been inferred from observations of dissolved iodine cycling near Bermuda and Hawaii, does not hold for the South Atlantic transect where minimum I^- concentrations are found in the regions with highest primary productivity. Instead, there seems to be a dependence of I^- concentrations on oceanic nitrate concentrations with a distinct anticorrelations between I^- and NO_3^- inside and outside the South Atlantic gyre. One explanation for this anticorrelation is the hypothesis that the phytoplankton uptake of IO_3^- involves nitrate reductase enzymes that reduce IO_3^- and NO_3^-. Higher nitrate concentrations, e.g., outside the gyres, would leave less nitrate reductase enzymes to reduce the IO_3^- resulting in lower I^- concentrations despite the higher primary productivity, and resulting in maximum I^- concentrations in the gyres where the maximum surface nutrient depletion occurs.

[18] The global oceanic nutrient climatology by *Louanchi and Najjar* [2000] from NCAR's Computational and Information System Laboratory research data archive (http://dss.ucar.edu) and I^--NO_3^- ratios from *Campos et al.* [1999] was used to infer the global distribution of monthly mean oceanic surface water (0 m depth) I^- concentrations. The I^- concentration inside the gyre was inferred using the relationship I^- [nM] = 106 – 29 $\times$ NO_3^- [μM] as reported by *Campos et al.* [1999, Table 1] for the subtropical gyre, whereas the I^- concentration outside the gyre was inferred using the relationship I^- [nM] = 70.4 – 2.12 $\times$ NO_3^- [μM], which reflects the average of the y intercept and slope of the other five observed relationships [*Campos et al.*, 1999]. A NO_3^- concentration below 2 μM was used to locate the gyres (Jim Butler, NOAA, Boulder, United States, personal communication, 2005).

[19] Figure 1 shows the inferred annual mean global distribution of oceanic I^- surface layer concentrations. Relatively high concentrations up to 100 nM are predicted for tropical and subtropical regions coinciding with the minimum NO_3^- concentrations inside the gyres, whereas smaller I^- concentrations <20 nM are seen at higher latitudes, e.g., the southern Atlantic and Pacific oceans. A comparison of these inferred I^- concentration fields with observed I^- data from *Truesdale et al.* [2000] is shown in Figure 2. These observations were collected during the 1996 Atlantic Meridional Transect Cruises 3 and 4 (AMT3 and AMT4), on board the RSS *James Clark Ross*, with the AMT3 cruise starting 22 September going south from the United Kingdom reaching the Falkland Islands at 14 October. The reverse transect, AMT4, was made between 21 April and 26 of May. Since only inorganic iodine and IO_3^- were measured, the I^- concentrations were estimated as the residual term. For the comparison we used the inferred I^- concentrations along the 20°W meridional transect from 50°N to 60°S taking the September/October (AMT3) and April/May (AMT4) average concentrations. The overall agreement between the observed and inferred I^- concentrations is reasonable, especially for the AMT4 cruise in the Southern Hemisphere (SH), whereas the inferred concentrations in the tropical and subtropical regions are on average 30% smaller compared to the AMT3 observations. The inferred concentrations do not show the observed decrease south of 40°S during AMT3 and north of $\sim$20°N for both cruises. This NH discrepancy can be explained by a

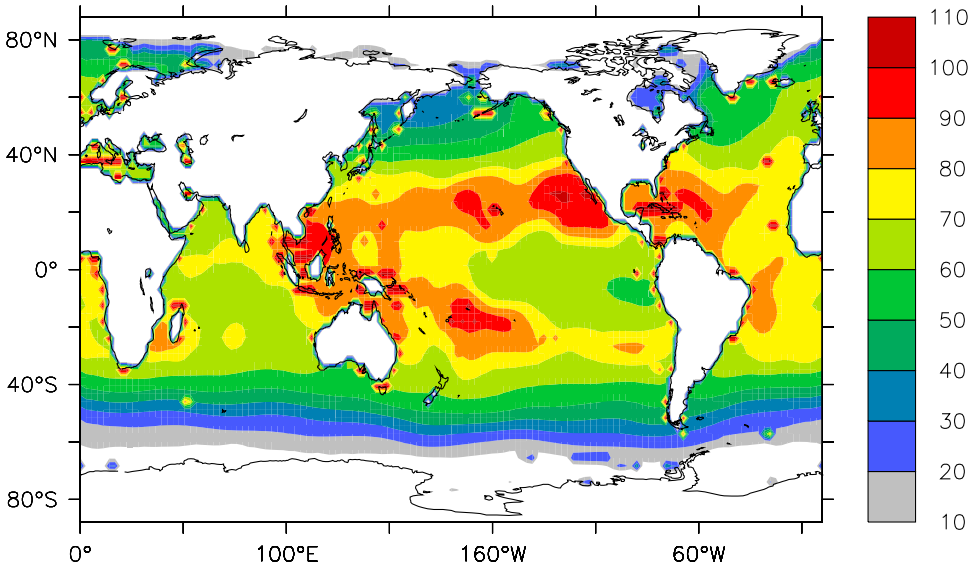

Figure 1. Global annual mean oceanic surface layer I^- concentration [nM] inferred from the oceanic surface layer NO_3^- climatology using the dependency described in the text.

relatively small gradient in the NO_3^- concentrations, which show a substantial increase exceeding 2 μM around 45N. Further analysis is required to assess if these discrepancies are due to differences between the actual and climatology NO_3^- concentrations or due to a limited applicability of the *Campos et al.* [1999] relationships. Inferred I^- concentrations are significantly lower compared to the observed concentrations near Hawaii and Bermuda, where observations show ~200–400 nM [*Campos et al.*, 1996]. However, those concentrations likely reflect the enhanced biological

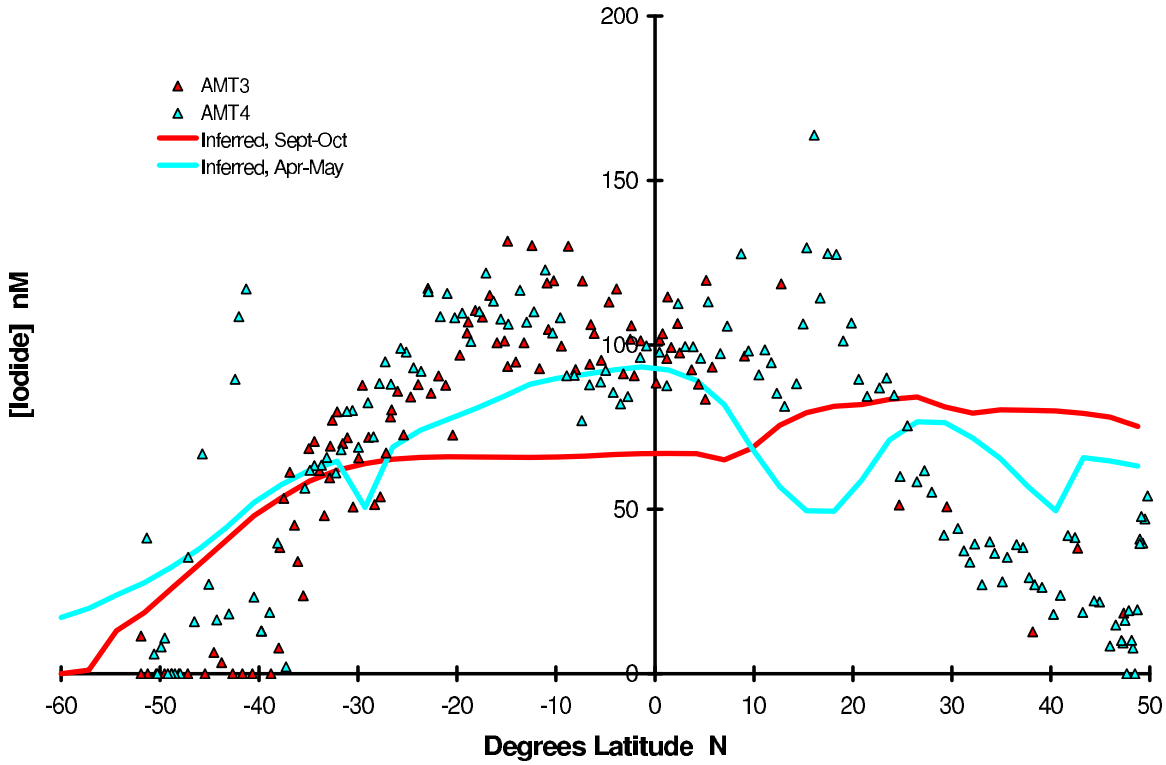

Figure 2. Comparison of the latitudinal gradient of inferred and observed oceanic surface layer I^- concentration [nM]. The mean of the September–October and April–May I^- concentrations for 20°W are compared with the observations collected during the AMT3 and AMT4 cruise, respectively.

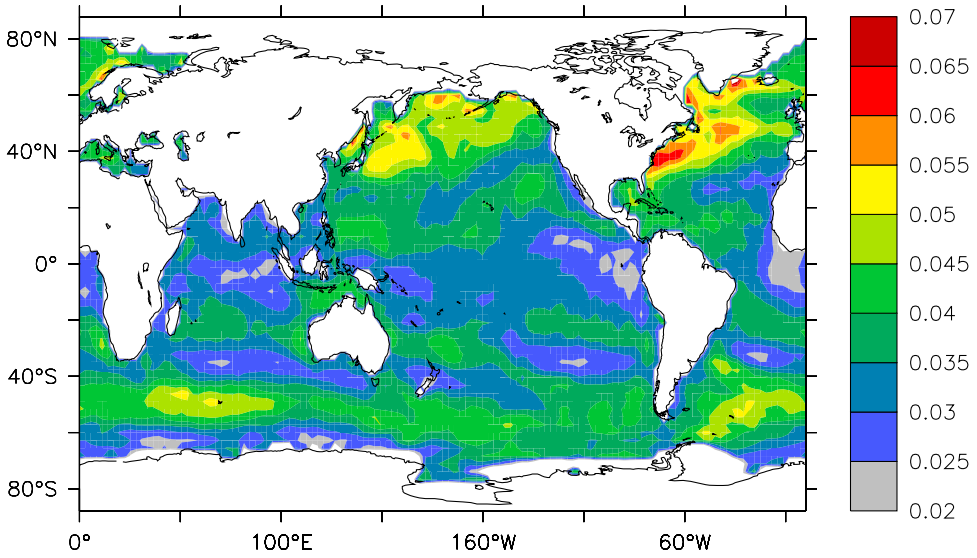

Figure 3a. January mean simulated oceanic O_3 dry deposition velocity (cm s^{-1}) based on the T-B oceanic ozone deposition model.

activity in coastal waters (Tim Jickells, School of Environmental Sciences, University of East Anglia, Norwich, United Kingdom, personal communication, 2005). These data resulted from measurements close to the islands, a feature that is not resolved in the global NO_3^- climatology, given its resolution on the order of 2 degrees. Similarly, the global chemistry-climate model, with a 2.8° spatial resolution (see section 5), is too coarse to reflect this feature. A recent study of the role of O_3 deposition in the air quality of the U.S. coastal region of the Gulf of Mexico by *Oh et al.* [2008] used a relationship with chlorophyll-*a* (CHL) based on observations of the water composition of a Brazilian bay [*Rebello et al.*, 1990] to infer I^-. Applying the linear dependence (slope of 0.231 μmol I^- per mg of CHL) and maximum observed CHL observations of 30 mg m^{-3} for the Gulf of Mexico (http://reason.gsfc.nasa.gov/OPS/Giovanni/ocean.seawifs.shtml) resulted in inferred I^- concentrations small as ~7 nM. In contrast, the $I^-NO_3^-$ relationship applied in our study results in significantly higher I^- concentrations of ~90 nM for the Gulf of Mexico.

[20] Despite the identified discrepancies the overall agreement in the inferred global I^- fields based on NO_3^- climatology appears to be satisfactory for a first-order assessment of the role of the oceanic I^- biogeochemistry in atmosphere-ocean O_3 exchange.

5. Evaluation of O_3 Deposition and Budget

5.1. Global Ozone Dry Deposition Velocities: Evaluation

[21] An evaluation of the O_3 dry deposition, concentrations and budgets calculated with the new O_3 oceanic dry deposition scheme (considering the role of waterside turbulence and biogeochemistry, hereafter referred to as "T-B" scheme) was done by comparing the simulations with available oceanic ozone flux measurements. As indicated in the introduction, there are only a limited number of O_3 dry deposition flux observations available for this purpose.

[22] Figures 3a and 3b show the global distribution in the simulated January and July mean oceanic V_{dO3}. These results show relatively large velocities of up to 0.1 cm s^{-1} over the higher-latitude storm track regions with V_{dO3} maxima reaching >0.2 cm s^{-1} for wind speeds >20 m s^{-1}. The minimum V_{dO3} in the high-latitude regions are as low as 0.01 cm s^{-1} during low wind speed conditions (<5 m s^{-1}) although there are substantial differences between the SH and NH high-latitude regions. The remarkable NH-SH differences reflect the different role of the biogeochemistry in these regions. The modeled V_{dO3} in tropical and subtropical regions is generally ~ 0.02–0.04 cm s^{-1} except for some regions, such as the northwestern Indian ocean in July with values >0.05 cm s^{-1}. The difference in the simulated annual maximum and minimum V_{dO3} (i.e., annual amplitude) is shown in Figure 4. There are large contrasts in annual variability in simulated V_{dO3} indicating two distinctly different regimes of oceanic O_3 deposition. There is a high temporal variability in V_{dO3} in midlatitude and high-latitude regions reflecting mostly the large temporal variability in wind speed and resulting role of atmospheric and waterside turbulent mixing in oceanic O_3 uptake. In contrast, in tropical and subtropical regions there is small temporal variability in V_{dO3} reflecting the more significant role of chemical enhancement in these regions and a relatively small role of waterside turbulence due to the year-round low wind speeds. The important role of chemical enhancement of O_3 oceanic uptake in tropical and subtropical regions is also indicated by minimum tropical and subtropical O_3 deposition velocities which are larger than the minimum V_{dO3} in midlatitude and high-latitude regions. The differences between the tropics and higher latitudes in terms of the role of biogeochemistry and turbulence in controlling the temporal variability as well as magnitude of

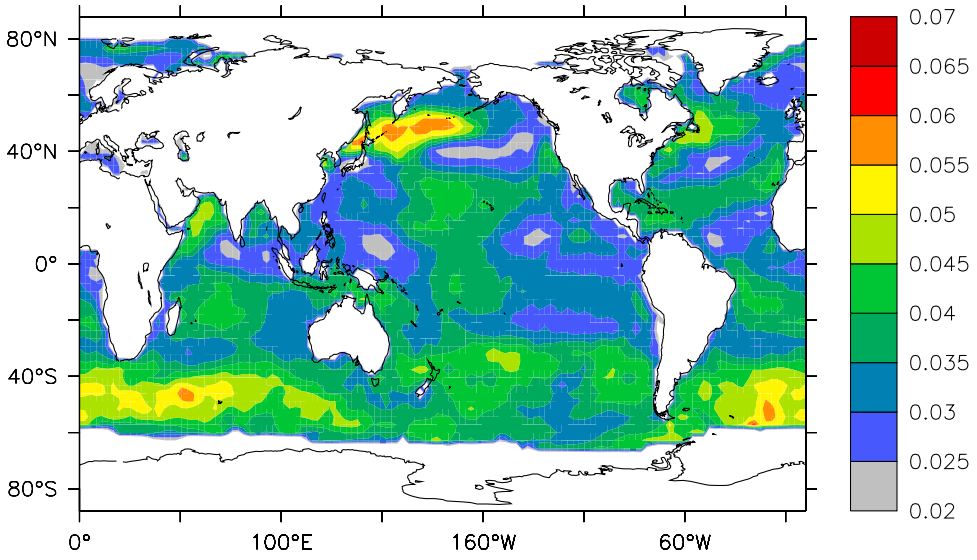

Figure 3b. July mean simulated oceanic O_3 dry deposition velocity (cm s^{-1}) based on the T-B oceanic ozone deposition model.

ozone oceanic water uptake are illustrated in Figure 5. It shows the simulated annual cycle in the O_3 ocean water uptake velocity (cm s^{-1}, the inverse of the water uptake resistance R_w in s m^{-1}) considering the role of only the biogeochemistry ($100/R_{wB}$) and considering the combined role of turbulence and biogeochemistry ($100/R_{wT\text{-}B}$) for two grid points 150°W at the Equator and 40°S. The annual mean O_3 ocean water uptake velocities for the two locations are not that different despite the fact that the nonturbulent uptake velocity is substantially smaller at 40°S compared to that at the Equator which results from a smaller reactivity at 40°S compared to that at the Equator. There is only a small temporal variability in the nonturbulent uptake velocity reflecting the combined effect of changes in solubility, controlled by the SST, and changes in the monthly mean I^- and DMS concentrations. The relatively high wind speeds at 40°S result in a substantial enhancement in the uptake efficiency and also introduce a much larger temporal variability in the uptake velocity compared to that at the Equator.

[23] Figure 6 shows the inferred annual mean global distribution in reactivity (summation of the products of the concentration of all species involved in O_3 destruction and the respective reaction rates). Comparison of this global distribution of reactivity with that of the oceanic I^- concentration, shown in Figure 1 indicates that in some regions

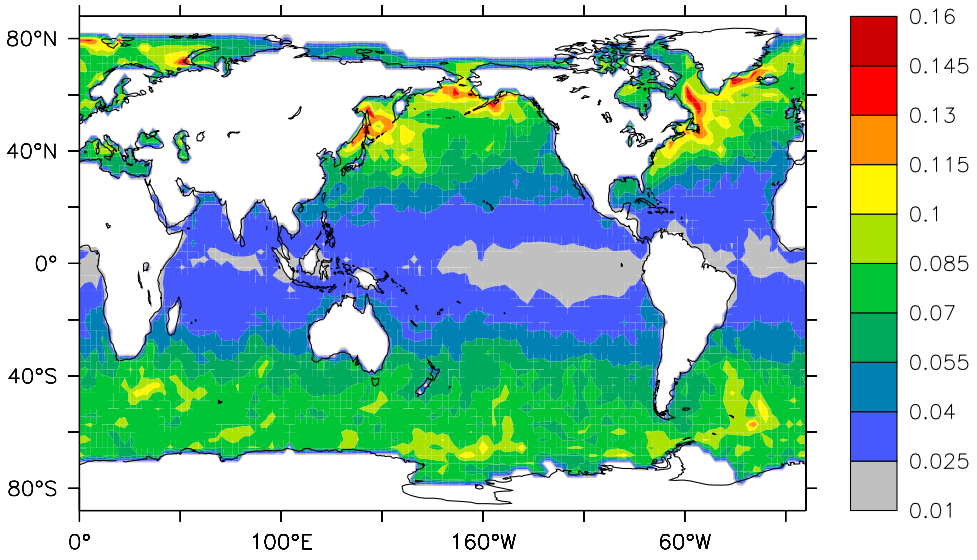

Figure 4. Difference between the annual maximum and minimum simulated V_{dO3} (cm s^{-1}) based on the T-B oceanic ozone deposition model.

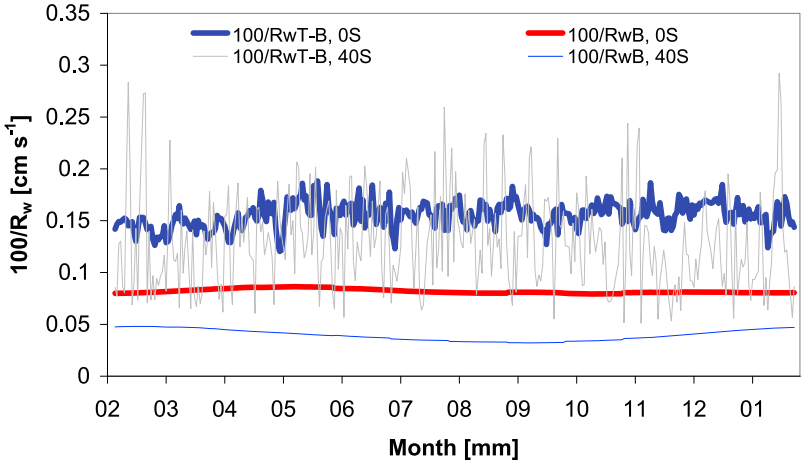

Figure 5. Annual cycle in O_3 oceanic uptake velocity (cm s^{-1}) (calculated from the water uptake resistance R_w including the role of turbulence ($R_{w\text{-}T\text{-}B}$) and without the role of turbulence ($R_{w\text{-}B}$) for two grid points both at 150°W. The thick and thin lines show the O_3 oceanic uptake velocity at the Equator and at 40°S, respectively. This annual cycle reflects a model output frequency of 25 h.

the spatial variability in reactivity correlates well with the I^- distribution, e.g., high reactivity and I^- concentrations in the SH Pacific east of the Fiji Islands, around the Asian Islands, west of Central America and in the southwest Atlantic. In other regions with high I^- concentrations, e.g., in the central and eastern subtropical Pacific, a substantial smaller reactivity reflects the dependence of reactivity on SST; the annual mean SST in this region is about 5K lower compared to the western Pacific. The potential large chemical enhancement in the tropical and subtropical regions is largely compensated by a smaller solubility due to the relative high SST. This results in an overall small temperature dependence of V_{dO3} as shown in Figure 7. Box model simulations with the T-B model for a wind speed of 7.5 m s^{-1} and I^- concentration of ~100 nM (see also Figure 2), reflecting a typical tropical/subtropical exchange regime, provide a nearly constant V_{dO3} of ~0.04 cm s^{-1} for a temperature range of 288–303K.

[24] In Table 2 we present a comparison of the calculated and observed O_3 dry deposition flux (F_{O3}) and V_{dO3} (inferred from the observed flux and concentration) for the few available field measurements of ozone atmosphere-water surface exchange. Note that for the coastal sites we used the simulated F_{O3} and V_{dO3} for the nearest grid with a sea cover fraction > 0.5 and used the mean, maximum and minimum simulated values of the month(s) covering the measurement period for the comparison. We also include a comparison with the measured O_3 dry

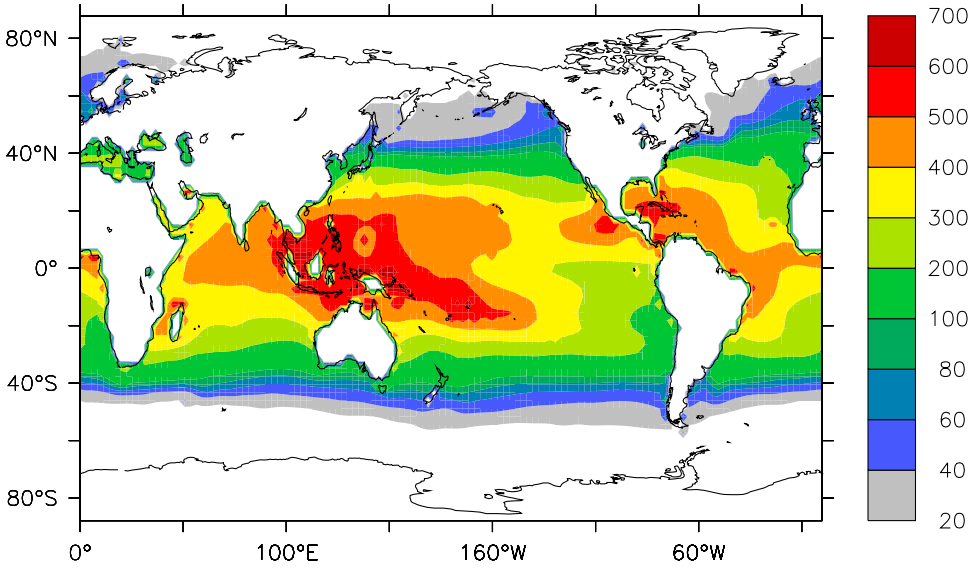

Figure 6. Annual mean simulated reactivity (s^{-1}). Note that the color bar scale is not linear, with smaller intervals being applied for a reactivity less then 100 s^{-1}.

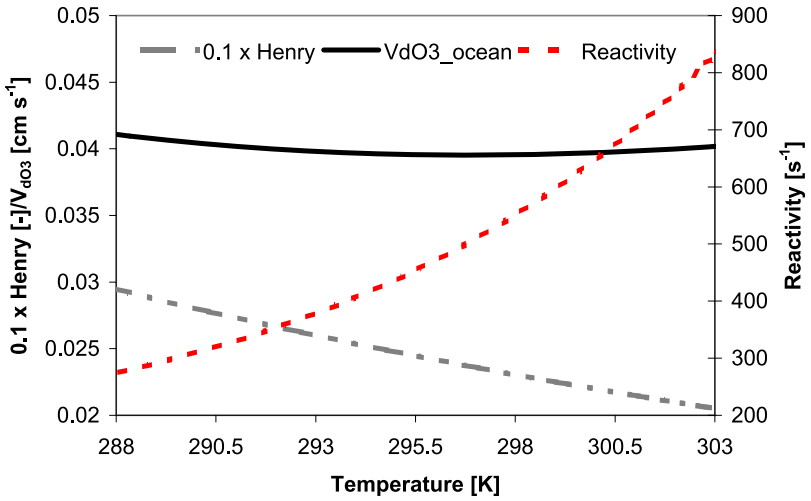

Figure 7. V_{dO3} (black line) as a function of SST reflecting conditions typical for tropical/subtropical regions, i.e., a wind speed of 7.5 m s^{-1} and an I^- concentration of 100 nM. Also shown are the changes in solubility, reflected by 0.1 × dimensionless Henry coefficient (gray dashed-dotted line) and reactivity (red dotted line) as a function of SST.

deposition fluxes to Lake Michigan by *Wesely et al.* [1981]. The comparison for this site indicates that the model overestimates V_{dO3}, which can be explained by a relatively small nonturbulent water uptake resistance (~1300 s m^{-1}). This efficient uptake by the lake water is caused by the inferred high DMS concentration in freshwater lakes, according to *Kettle and Andreae* [2000], which at 200 nM is much larger than the typical oceanic concentrations of <20 nM. The comparison of the oceanic observations by *Kawa and Pearson* [1989] and *Heikes et al.* [1996] (note that in the later study the O_3 flux and dry deposition velocity was inferred from the MBL budgets) over rather remote large areas show a good agreement between the simulated and observed flux and deposition velocity values. The average simulated V_{dO3} over these areas, the eastern subtropical Pacific, and (sub) tropical Atlantic and western Indian Ocean, is smaller compared to the value of ~0.05 cm s^{-1} used in previous global model approaches. The simulated small temporal variability (indicated by difference between the minimum and maximum V_{dO3}) in these regions reflects a more important role of biogeochemistry compared to turbulent transfer. The model significantly underestimates the observed V_{dO3} at the coastal sites in the North Sea. Note that these observed V_{dO3}'s reflect the surface uptake velocity, excluding the atmospheric transport velocity, which is generally much faster compared to the limiting ocean surface uptake rate. The difference between the simulated nonturbulent (~2400 s m^{-1}) and turbulent surface uptake resistance (~1100 s m^{-1}) at the U.K. coastal site suggests that the simulated June O_3 dry deposition for this site is strongly enhanced by waterside turbulence. Consequently, a too small simulated average (June) friction velocity (u*) of 0.14 m s^{-1}, compared to the observed typical u* of 0.21 m s^{-1}, also partly explains the discrepancy between the simulated and observed V_{dO3}. However, *Fairall et al.* [2007, Figure 2] show that a substantially larger reactivity (i.e., >1000 s^{-1}) compared to our inferred reactivity of 84 s m^{-1} is required to reach the observed V_{dO3} of about 0.1 cm s^{-1}.

[25] The limited number of in situ oceanic ozone flux measurements, with two of those [*Tiefenau and Fabian*, 1972; *Gallagher et al.*, 2001] representing rather local conditions in terms of turbulence and biogeochemistry, poses a serious limitation for drawing any firm and more quantitative conclusions. The latter requires oceanic ozone fluxes measurements representative for open ocean conditions at scales comparable to that of large-scale model including observations of key meteorological as well as biogeochemical drivers.

[26] Two additional simulations were conducted to assess the potential enhancement in O_3 ocean uptake associated with iodide-ozone chemistry as well as organic chemistry. In one simulation we used a significantly larger I^- concentration of 300 nM (in the middle of the range observed by *Campos et al.* [1996] close to Hawaii and Bermuda; see section 4) for coastal zones. Coastal zones were inferred from an ocean bathymetric data set using a threshold depth of 200m. Such elevated concentrations of I^- only provide significantly enhanced reactivities (>1000 s^{-1}) in tropical and subtropical coastal zones, e.g., around the Indonesian islands. However, for those locations O_3 oceanic uptake is not limited by the I^--O_3 interaction but rather by a small solubility due to high SST as discussed previously (see Figure 7). On the other hand, in the midlatitude to high-latitude coastal zones, e.g., at the U.K. coastal site in June, an assumed enhanced coastal water I^- concentration does not result in a substantial increase in V_{dO3} since here the oceanic uptake is limited by relative small O_3-I^- reaction rates due to a relative low SST. These results are rather contrasting to those by *Oh et al.* [2008] who found a strong enhancement in V_{dO3} in U.S. coastal regions associated with elevated I^- concentrations. Our analysis suggests that consideration of the SST in solubility and reactivity seems

Table 2. Observed and Simulated O_3 Fluxes and Dry Deposition Velocities With the New O_3 Ocean Dry Deposition Scheme[a]

		F_{O3} (1e-15 molec m^{-2} s^{-1})		V_{dO3} (cm s^{-1})			$V_{dO3\text{-}CHL}$ (cm s^{-1})	
Reference	Location	Obs.	Model	Obs.	Model	Obs.-Model	Model	Obs.-Model
Tiefenau and Fabian [1972]	Coastal zone, North Sea	–	0.35	0.08–0.15*	0.034 (0.001–0.070)	0.091	0.082	0.043
Wesely et al. [1981]	Lake Michigan	0.16	0.72	0.004–0.02	0.034 (0.002–0.076)	−0.024	0.034	−0.024
Lenschow et al. [1982]	Gulf of Mexico	1.025–1.223	0.28	0.05	0.032 (0.020–0.039)	0.018	0.070	−0.020
	North Pacific Ocean	0.58	0.47	0.06	0.041 (0.013–0.067)	0.019	0.046	0.014
Kawa and Pearson [1989]	East Pacific	0.19 (0.1–0.26)	0.33	0.02	0.033 (0.023–0.041)	−0.013	0.035	−0.015
Heikes et al. [1996]	South Atlantic	0.17	0.78	0.03	0.022 (0.018–0.025)	0.008	0.024	0.006
Gallagher et al. [2001]	Coastal zone, North Sea	~2.5	0.44	0.1 (0.01–0.14)*	0.031 (0.005–0.048)	0.069	0.093	0.007

[a]The observed V_{dO3} is presented as the mean or the observed range whereas the simulated V_{dO3} reflect the monthly mean (and the minimum and maximum values) for the months during which the observations were collected. Also shown are the differences between the observations and the model. The * denotes observed surface uptake velocities, which excludes the role of turbulent transport to the ocean surface. The last two columns reflect the simulated V_{dO3} including the chlorophyll-ozone reactions ($V_{dO3\text{-}CHL}$), only showing the monthly mean, as well as the differences between the observations and the model.

to substantially reduce the sensitivity of V_{dO3} to enhanced I^- concentrations in coastal waters.

[27] The observed relative high V_{dO3} for the North Sea coastal sites suggest a potential important role of organic chemistry. Observed annual mean chlorophyll concentrations, taken from the World Ocean Atlas 2001 database (http://www.nodc.noaa.gov/OC5/WOA01/woa01dat.html) show relative high chlorophyll concentrations (>2 ug l^{-1}) for the North Sea. In order to assess the possible role of the organic chemistry in oceanic O_3 deposition we conducted an experiment in which we used the global seasonal distribution of oceanic CHL concentrations. We applied a CHL-O_3 reactivity that linearly increases with the chlorophyll concentration such that the model simulates a factor 2–3 enhancement in V_{dO3} for maximum chlorophyll concentrations as observed by *Clifford et al.* [2008]. Inclusion of this CHL-O_3 aqueous phase chemistry must be interpreted as a first-order approximation of the role of dissolved organic matter (DOM) in oceanic O_3 dry deposition at a global scale. We recognize that this is a crude simplification of the extremely complex interactions between all oceanic organic compounds relevant to oceanic ozone uptake. On the other hand, it cannot be expected that, besides the observed chlorophyll-ozone reaction rates, the full range of chemical interactions involved in DOM-O_3 interactions can be quantified explicitly. As such this analysis provides a first insight in the potential importance of the role of organic chemistry in global oceanic O_3 dry deposition for guidance in further experimental studies focusing on this theme.

[28] Figure 8 shows box model simulations of V_{dO3} as a function of temperature comparing V_{dO3} considering the I^-, DMS and alkene chemistry (V_{dO3}) only, and including the CHL-O_3 chemistry ($V_{dO3+CHL}$). These simulations reflect a prescribed wind speed of 7.5 m s^{-1}, an I^- concentration of 100 nM; the CHL-O_3 reactivity simulation uses a chlorophyll concentration of 10 ug l^{-1}. The stronger decrease in

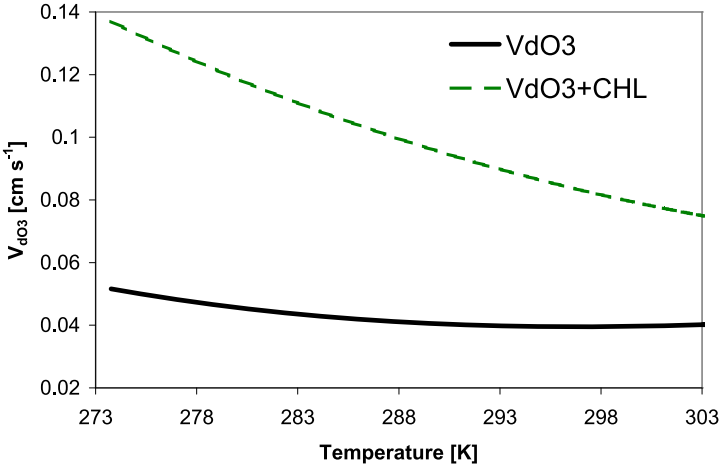

Figure 8. V_{dO3} for I^-, DMS and alkene chemistry (black line) and adding CHL-O_3 reactivity (green dashed-dotted line) as a function of temperature, ranging from 273 to 303K, for a wind speed of 7.5 m s^{-1}, I^- concentration of 100 nM and chlorophyll concentration of 10 ug l^{-1}.

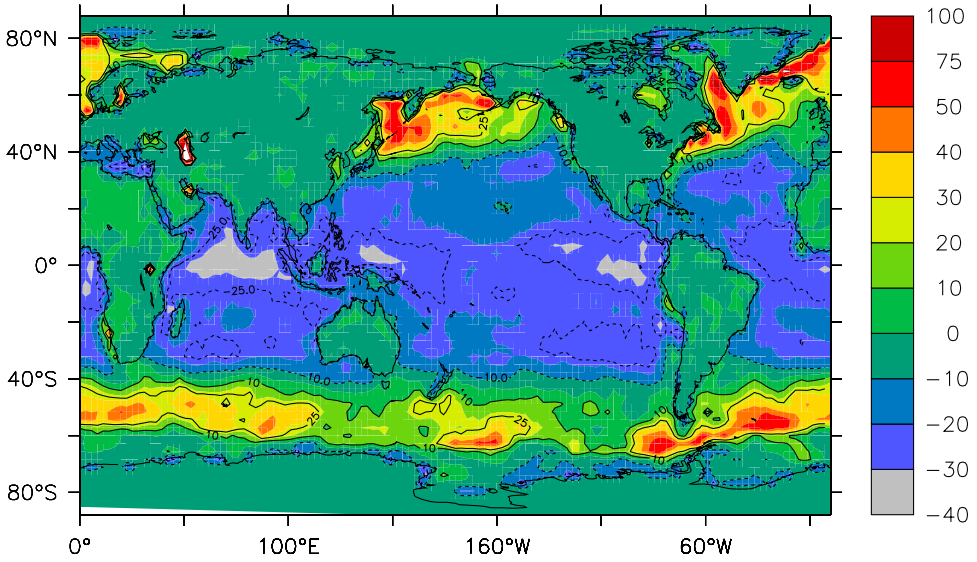

Figure 9. Annual mean relative difference (%) between the $ConstR_s$ and T-B_{+CHL} O_3 flux (calculated as 100 × (T-B_{+CHL} − $ConstR_s$)/$ConstR_s$) with positive values indicating a larger simulated T-B_{+CHL} O_3 deposition flux simulated compared to the $ConstR_s$ scheme and vice versa. The −25%, −10% (dashed lines) and 10% and 25% (solid lines) contours are also shown; the white areas indicate relative differences outside the range. Note that the scale is not linear; larger intervals are used for relative changes >50%.

$V_{dO3+CHL}$ compared to that in V_{dO3} with an increase in temperature is explained by the temperature-independent CHL-O_3 reaction rate and, consequently, the missing compensation for the decrease in solubility with an increase in temperature.

[29] The impact of adding this CHL-O_3 reactivity to the I^--, DMS- and alkene-O_3 reactivity on the simulation of oceanic O_3 deposition is also presented in Table 2. Note that for the North Sea coastal sites, we used the simulated $V_{dO3+CHL}$ for a grid in the middle of the North Sea since, due to the relative coarse resolution of the model, the interpolation between land and ocean grid squares result in substantially smaller (∼ factor 2) chlorophyll concentrations for the coastal grid points compared to the maximum concentrations of the input data set. Including the CHL-O_3 chemistry results in a substantial increase in V_{dO3} and better agreement with the observations for the North Sea. But the inclusion of the chlorophyll-O_3 chemistry also increases V_{dO3} for the Gulf of Mexico as well as for the U.S. Atlantic coast resulting in an overestimation of the simulated V_{dO3} compared to the *Lenschow et al.* [1982] observations. For the more remote sites, e.g., the eastern Pacific, there are only small changes due to the small CHL concentrations in that region. Overall, the reasonable agreement between the simulated and observed O_3 dry deposition velocities for the three open ocean areas [*Lenschow et al.*, 1982; *Kawa and Pearson*, 1989; *Heikes et al.*, 1996], with or without CHL-O_3 chemistry, suggests that the considered waterside turbulence and I^-, DMS and alkenes chemistry seem to sufficiently explain the ozone uptake for these sites. In addition, the reasonable agreement between simulated and observed O_3 deposition fluxes, the product of V_{dO3} and the surface layer concentration, indicates that the chemistry-climate model captures well the O_3 surface layer concentrations at these remote sites. This evaluation of V_{dO3} using the parameterized CHL-O_3 reactivity shows the potential role of the organic chemistry in oceanic ozone deposition to the oceans. However, at this time it is difficult to draw more firm conclusions about this possible influence on oceanic O_3 dry deposition due to the sparseness of available in situ ocean flux observations, oceanic biogeochemical properties, as well as quantifiable DOM-O_3 chemical interactions beyond those reported for chlorophyll.

5.2. Ozone Dry Deposition Fluxes and Concentrations

[30] Figure 9 shows the annual mean relative differences in the O_3 oceanic dry deposition fluxes based on the constant surface uptake resistance scheme (hereafter referred to as "$ConstR_s$" scheme), and the fluxes calculated according to the T-B scheme (including the CHL-O_3 chemistry). There are both significant relative increases as well as decreases in the T-B_{+CHL} O_3 dry deposition fluxes compared to those calculated with the $ConstR_s$ scheme. Large relative increases > 50% in O_3 dry deposition fluxes with the T-B_{+CHL} scheme are found in temperate and high-latitude regions with some of these located downwind of regions with high ozone concentrations and large oceanic O_3 dry deposition fluxes, e.g., east of the North American and Asian coasts. These large increases in ozone deposition mainly reflect the role of O_3−CHL interactions. A comparison of the regions with largest increases in O_3 deposition with the global distribution of CHL that we applied in our analysis (World Ocean Atlas 2001 database), indicates that the T-B_{+CHL} scheme calculates substantially larger O_3 deposition fluxes than the $ConstR_s$ scheme in temperate to high-latitude regions where chlorophyll concentrations

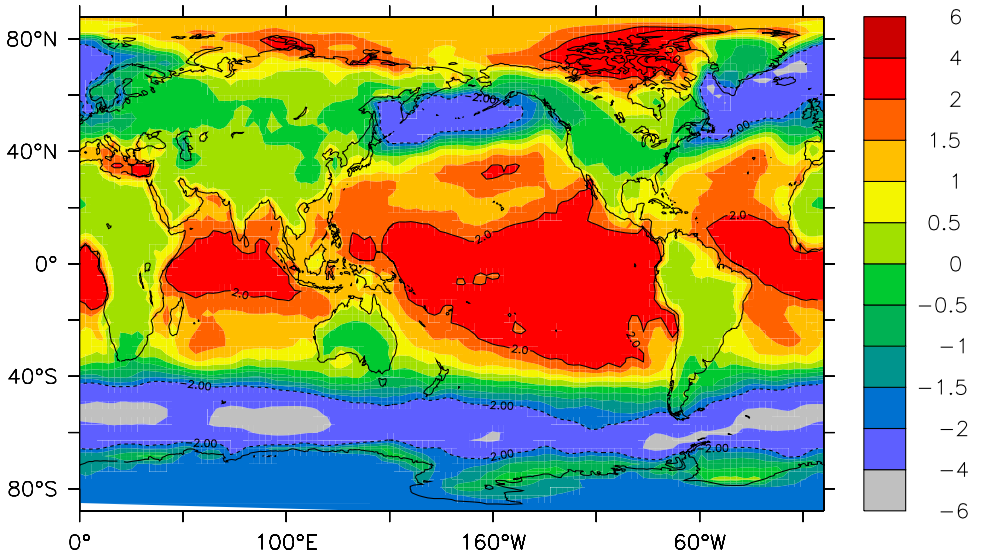

Figure 10. Annual mean relative differences in Marine Boundary Layer O_3 mixing ratios (%) between the $ConstR_s$ and $T\text{-}B_{+CHL}$ scheme with positive values indicating an increase in mixing ratio due to a decrease in deposition in the $T\text{-}B_{+CHL}$ dry deposition scheme compared to the $ConstR_s$ scheme and vice versa. Also shown are the −2% (dashed line) and +2% (solid line) contours.

> 0.5 ug l^{-1}. Such enhanced chlorophyll concentrations do not result in a substantial increase in tropical ozone deposition, e.g., to the eastern tropical Pacific, due to the limiting role of turbulence and solubility. Despite the inclusion of enhanced reactivity associated with the CHL-O_3 reaction the simulations actually show substantially smaller O_3 deposition up to about −40% for the tropical and subtropical oceans compared to the $ConstR_s$ scheme.

[31] In order to demonstrate the impact of these changes in oceanic ozone deposition on ozone concentrations we show in Figure 10 the relative differences in the annual mean MBL mixing ratios between the $T\text{-}B_{+CHL}$ and $ConstR_s$ scheme. Despite maximum differences in V_{dO3} between the two schemes of ∼0.05 cm s^{-1}, simulated differences between the $T\text{-}B_{+CHL}$ and $ConstR_s$ MBL annual mean O_3 mixing ratios are surprisingly low and generally <5% over most of the oceans. In regions with a relative high O_3 uptake from efficient turbulent transport and CHL-O_3 reactivity, e.g., the Southern Ocean storm tracks and northeast of Asia and North America, we simulate maximum decreases in the annual mean O_3 mixing ratios of 2.5−5%. The decrease in tropical oceanic O_3 deposition results in a simulated increase in O_3 over the eastern tropical Pacific of <4%.

[32] These changes in ozone express a substantially smaller sensitivity of boundary layer ozone to oceanic ozone deposition compared to the MATCH-MPIC sensitivity analysis despite the fact that the maximum differences in the simulated V_{dO3} between the $T\text{-}B_{+CHL}$ and $ConstR_s$ scheme are comparable to the applied range in the $ConstR_s$ V_{dO3} values applied in the MATCH-MPIC sensitivity analysis. The smaller sensitivity of simulated O_3 concentrations points at the importance of compensating effects associated with oceanic ozone uptake, atmospheric transport (advection and turbulence) and chemistry. For example, the inferred relative high I^- concentrations and relatively strong chemical enhancement in tropical and subtropical oceans compensate for a reduced solubility and atmospheric and waterside turbulent mixing from the high SST and low wind speeds, respectively. On the other hand, the relatively small role of O_3-I^- chemistry at higher latitudes is not only compensated for by the enhanced waterside turbulence but also by the enhanced amount of organic matter in these regions. The efficient removal of ozone at high wind speeds is compensated for by an extra supply of ozone through horizontal and vertical transport (see below).

[33] Small changes in annual mean MBL O_3 mixing ratios due to the explicit calculation of the oceanic surface uptake resistance are associated with relative small changes in the global annual mean dry deposition budget. Table 3 shows that implementation of the explicit oceanic O_3 dry deposition scheme, including the CHL-O_3 chemistry results in a decrease of 6% in oceanic ozone deposition and a negligible change in the global O_3 dry deposition budget (0.5%) compared to the commonly applied constant uptake rate approach. This change in O_3 oceanic uptake of ∼17 Tg O_3 yr^{-1} is mostly compensated for by transport and not by transport and atmospheric chemistry. This can be inferred from a difference in the global boundary layer mass budget of net chemical production/destruction of O_3 between the $T\text{-}B_{+CHL}$ and $ConstR_s$ scheme small as ∼2 Tg O_3 yr^{-1}

Table 3. Global and Oceanic Dry Deposition Budgets Calculated With the $ConstR_s$ and the $T\text{-}B_{+CHL}$ O_3 Dry Deposition Scheme[a]

	$ConstR_s$	$T\text{-}B_{+CHL}$
Global O_3 dep. (Tg yr^{-1})	837	833 (−0.5%)
Marine O_3 dep. (Tg yr^{-1})	300	283 (−6%)

[a]The relative changes between the two schemes, calculated as 100 × $(T\text{-}B_{+CHL} - ConstR_s)/(ConstR_s)$, are indicated in parentheses.

suggesting that for mass balance ($dM = dM_{dry\ deposition} + dM_{transport} + dM_{chemistry}$) the remaining difference of 15 Tg O_3 yr^{-1} is due to changes in transport. The global average O_3 ocean dry deposition velocity of about 0.044 cm s^{-1} simulated with the T-B_{+CHL} scheme, is very close to the global annual average of the ConstR_s scheme of 0.047 cm s^{-1}. Solely based on these comparable global annual mean V_{dO3} one could draw the conclusion that the commonly applied ConstR_s approach (using an R_s of 2000 s m^{-1}) seems to provide a good first-order estimate of global and long-term average oceanic ozone dry deposition for use in atmospheric chemistry and transport models. Nonetheless, we recommend applying the more mechanistic oceanic ozone uptake to account for the temporal and spatial variability in oceanic ozone deposition as simulated by the T-B_{+CHL} scheme to properly consider the importance of compensating effects for tropospheric ozone.

6. Conclusions and Outlook

[34] We implemented a mechanistic representation of oceanic ozone dry deposition in a chemistry-climate model. This model incorporates the role of biogeochemistry and turbulent and diffusive transfer in oceanic ozone deposition. The dry deposition scheme considers, in addition to atmospheric turbulent mixing, also turbulent and molecular diffusive transfer in the oceanic surface layer and enhancement of exchange via whitecap-generated bubbles. It also considers explicitly the role of ocean biogeochemistry in the form of first-order estimates of the chemical destruction of O_3 through its reaction with I^-, DMS and alkenes, and temperature-dependent solubility and reaction rates. We have also presented the important role of organic chemistry in oceanic O_3 dry deposition considering the chlorophyll-ozone chemical interaction as proxy for the role of DOM-O_3 reactivity in oceanic ozone uptake.

[35] Analyses that exclude the role of chlorophyll-O_3 interactions reveal two distinctly different removal regimes between tropical and subtropical regions, with an important role of biogeochemistry in ozone chemical destruction in the tropics, and an enhanced influence of turbulent mixing and diffusion at higher latitudes. Evaluation of the model using the limited number of observations over the open ocean indicates that the most efficient chemical destruction mechanism, which is the I^--O_3 reaction, already sufficiently enhances O_3 uptake such that the simulated V_{dO3} yields a reasonable agreement with the observations. Underestimation of the simulated V_{dO3} for the coastal sites, even assuming elevated coastal water I^- concentrations, suggests that the model lacks an important contribution to the enhancement in oceanic ozone uptake near the coasts. This enhanced reactivity could potentially be associated with reactions of ozone with organic material.

[36] The analysis that includes the chlorophyll-ozone reactivity indicates that this particular contribution to the DOM-O_3 chemical interactions can explain the coastal observations of V_{dO3}. A more extensive evaluation to substantiate these findings requires open ocean observations representative for a spatial scale comparable to the model resolution, i.e., the chemistry-climate model, and/or the resolution of the input databases that have been applied to define the biogeochemical boundary conditions in the model.

[37] It appears that there are a remarkable number of compensating effects that determine the spatial and temporal variability in oceanic ozone uptake. The impact of the new oceanic O_3 dry deposition scheme on the oceanic O_3 sink is significant whereas the impact on MBL concentrations is small. These findings are in strong contrast with a sensitivity analysis based on the commonly applied global constant ocean uptake approach which demonstrated significant changes in O_3 deposition and mixing ratios using a range of observed O_3 uptake rates. Despite large and highly variable O_3 dry deposition velocities in high-latitude regions, associated with high wind speeds, decreases in MBL O_3 concentrations are small compared to the constant surface uptake scheme as a result of compensating effects associated with atmospheric transport and chemistry. In contrast, in tropical and subtropical regions the explicitly simulated surface uptake rate, which shows a small temporal and spatial variability reflecting a more important role of the biogeochemistry, results in a simulated mean V_{dO3} for these regions of about 0.02–0.03 cm s^{-1}. This is about half the value used in the constant surface uptake scheme V_{dO3}. This decrease in ozone removal results in an increase in the MBL O_3 concentrations generally <5%. Obviously, through the inclusion of the role of waterside turbulence and biogeochemistry in oceanic ozone uptake these compensating effects are more properly accounted for in atmospheric chemistry and transport models. It warrants a more realistic analysis of the role of the oceans in ozone exchange and atmospheric chemistry and, more generally, points at the relevance of mechanistic modeling of gas exchange for climate sensitivity analysis. Model simulations that do not consider the explicit mechanisms, i.e., those involved in ocean-atmosphere O_3 exchange, will reflect a too large sensitivity of O_3, and consequently of the role of O_3 in climate, to variability in atmospheric processes.

[38] This study also underscores the need for open ocean field observations that reflect contrasting exchange regimes with a different role of atmospheric and waterside turbulence as well as biogeochemistry. Such measurements are urgently needed to further examine the dependencies of oceanic ozone uptake as addressed in this analysis. We suggest that future measurements of ocean-atmosphere O_3 exchange should preferably be conducted in the temperate coastal zones known to show a large variability in organic matter and downwind of the continental regions with elevated concentrations of ozone, e.g., the east coast of the United States and Asia. These campaigns should include detailed micrometeorological measurement along with detailed physical and biogeochemical properties and compounds of importance to the air-sea exchange of ozone. Characterization of the oceanic biogeochemical controls will assist in quantifying the contribution of iodide and organic chemistry to the O_3 uptake by the ocean. Moreover, based on the discussed relationship between O_3 uptake, the oxidation of DOM and potential resulting oceanic VOC emissions, it would be valuable to conduct concurrent flux measurements of VOC and O_3 oceanic

exchange and ocean water DOM measurements to further examine these dependencies.

[39] **Acknowledgments.** We acknowledge the contribution by Rolf von Kuhlmann, now at DLR, Bonn, Germany, for conducting the sensitivity analysis with the MATCH-MPIC model. We also greatly appreciate access to the oceanic iodide observations, collected during the Atlantic Meridional Transect Cruises. These data were provided by Vic Truesdale at CCMS, Plymouth Marine Laboratory, Plymouth, United Kingdom. We would like to thank Jim Butler, NOAA, Boulder, United States, for his input on the use of ocean biogeochemical data sets and Roland von Glasow, School of Environmental Sciences, University of East Anglia, Norwich, United Kingdom, and Jonathan Williams of the Max Planck Institute for Chemistry, Mainz, Germany, for their constructive comments. We also want to express our appreciation to all the MPI-C colleagues that contributed to the development of the MESSy model system. Finally, we want to thank two reviewers for their constructive comments. This work has been supported by the U.S. National Science Foundation, research grant OCE 0410058. Any opinions, findings, and conclusions expressed in this material are those of the authors and do not necessarily reflect the views of the National Science Foundation.

References

Aldaz, L. (1969), Flux measurements of atmospheric ozone over land and water, *J. Geophys. Res.*, *74*, 6943–6946.

Antoine, D., J.-M. Andre, and A. Morel (1996), Oceanic primary production: 2. Estimation at global scale from satellite (coastal zone cooler scanner) chlorophyll, *Global Biogeochem. Cycles*, *10*, 57–69, doi:10.1029/95GB02832.

Bariteau, L., D. Helmig, C. W. Fairall, J. E. Hare, J. Hueber, and E. K. Lang (2009), Determination of oceanic ozone deposition by ship-borne eddy covariance flux measurements, *Atmos. Meas. Tech. Discuss.*, *2*, 1933–1972.

Bey, I., D. J. Jacob, R. M. Yantosca, J. A. Logan, B. D. Field, A. M. Fiore, Q. B. Li, H. G. Y. Liu, L. J. Mickley, and M. G. Schultz (2001), Global modeling of tropospheric chemistry with assimilated meteorology: Model description and evaluation, *J. Geophys. Res.*, *106*, 23,073–23,095, doi:10.1029/2001JD000807.

Brasseur, G. P., D. A. Hauglustaine, S. Walters, P. J. Rasch, J. F. Muller, C. Granier, and X. X. Tie (1998), MOZART, a global chemical transport model for ozone and related chemical tracers: 1. Model description, *J. Geophys. Res.*, *103*, 28,265–28,289, doi:10.1029/98JD02397.

Broadgate, W. J., P. S. Liss, and S. A. Penkett (1997), Seasonal emissions of isoprene and other reactive hydrocarbon gases from the ocean, *Geophys. Res. Lett.*, *24*, 2675–2678, doi:10.1029/97GL02736.

Campos, M. L. A. M., A. M. Farrenkopf, T. D. Jickells, and G. W. Luther III (1996), A comparison of dissolved iodine cycling at the Bermuda Atlantic Time-series Station and Hawaii Ocean Time-series Station, *Deep Sea Res., Part II*, *43*, 455–466, doi:10.1016/0967-0645(95)00100-X.

Campos, M. L. A. M., R. Sanders, and T. Jickells (1999), The dissolved iodate and iodide distribution in the South Atlantic from the Weddel Sea to Brazil, *Mar. Chem.*, *65*, 167–175, doi:10.1016/S0304-4203(98)00094-2.

Chang, W., B. G. Heikes, and M. Lee (2004), Ozone deposition to the sea surface: Chemical enhancement and wind speed dependence, *Atmos. Environ.*, *38*, 1053–1059, doi:10.1016/j.atmosenv.2003.10.050.

Ciccioli, P., E. Brancaleoni, A. Cecinato, and A. Brachetti (1993), Ubiquitous occurrence of semi-volatile carbonyl compounds in the troposphere and their possible sources, *Atmos. Environ.*, *27*, 1891–1901.

Clifford, D., D. J. Donaldson, M. Brigante, B. D'Anna, and C. George (2008), Reactive uptake of ozone by chlorophyll at aqueous surfaces, *Environ. Sci. Technol.*, *42*, 1138–1143, doi:10.1021/es0718220.

Dowideit, P., and C. von Sonntag (1998), Reaction of ozone with ethene and its methyl- and chlorine-substituted derivatives in aqueous solution, *Environ. Sci. Technol.*, *32*, 1112–1119, doi:10.1021/es971044j.

Fairall, C. W., J. E. Hare, J. B. Edson, and W. McGillis (2000), Parameterization and micrometeorological measurement of air-sea gas transfer, *Boundary Layer Meteorol*, *96*, 63–105, doi:10.1023/A:1002662826020.

Fairall, C. W., D. Helmig, L. Ganzeveld, and J. Hare (2007), Water-side turbulence enhancement of ozone deposition to the ocean, *Atmos. Chem. Phys.*, *7*, 443–451.

Fan, S.-M., S. C. Wofsky, P. S. Bakwin, D. J. Jacob, and D. R. Fitzjarrald (1990), Atmosphere-biosphere exchange of CO_2 and O_3 in the central Amazon forest, *J. Geophys. Res.*, *95*, 16,851–16,864, doi:10.1029/JD095iD10p16851.

Galbally, I. E., and C. R. Roy (1980), Destruction of ozone at the Earth's surface, *Q. J. R. Meteorol. Soc.*, *106*, 599–620, doi:10.1002/qj.49710644915.

Gallagher, M. W., K. M. Beswick, and H. Coe (2001), Ozone deposition to coastal waters, *Q. J. R. Meteorol. Soc.*, *127*, 539–558, doi:10.1002/qj.49712757215.

Ganzeveld, L., and J. Lelieveld (1995), Dry deposition parameterization in a chemistry general circulation model and its influence on the distribution of reactive trace gases, *J. Geophys. Res.*, *100*, 20,999–21,012.

Ganzeveld, L., J. Lelieveld, and G. J. Roelofs (1998), Dry deposition parameterization of sulfur oxides in a chemistry and general circulation, *J. Geophys. Res.*, *103*, 5679–5694, doi:10.1029/97JD03077.

Ganzeveld, L., J. Lelieveld, F. J. Dentener, M. C. Krol, A. J. Bouwman, and G.-J. Roelofs (2002), Global soil-biogenic NO_x emissions and the role of canopy processes, *J. Geophys. Res.*, *107*(D16), 4298, doi:10.1029/2001JD001289.

Garland, J. A., and S. A. Penkett (1976), Absorption of peroxy acetyl nitrate and ozone by natural surfaces, *Atmos. Environ.*, *10*, 1127–1131.

Garland, J. A., A. W. Elzerman, and S. A. Penkett (1980), The mechanism for dry deposition of ozone to seawater surfaces, *J. Geophys. Res.*, *85*, 7488–7492, doi:10.1029/JC085iC12p07488.

Gershenzon, M., D. Davidovits, J. T. Jayne, C. E. Kolb, and D. R. Worsnop (2001), Simultaneous uptake of DMS and ozone on water, *J. Phys. Chem.*, *105*, 7031–7036.

Greenberg, J. P., and P. R. Zimmerman (1984), Nonmethane hydrocarbons in remote tropical, continental, and marine atmospheres, *J. Geophys. Res.*, *89*, 4767–4778, doi:10.1029/JD089iD03p04767.

Hansell, D. A., and C. A. Carlson (2001), Marine dissolved organic matter and the carbon cycle, *Oceanography*, *14*, 41–49.

Hare, J. E., C. W. Fairall, W. R. McGillis, B. Ward, and R. Wanninkhof (2004), Evaluation of the National Oceanic and Atmospheric Administration/Coupled-Ocean Atmospheric Response Experiment (NOAA/COARE) air-sea gas transfer parameterization using GasEx data, *J. Geophys. Res.*, *109*, C08S11, doi:10.1029/2003JC001831.

Heikes, B., M. H. Lee, D. Jacob, R. Talbot, J. Bradshaw, H. Singh, D. Blake, B. Anderson, H. Fuelberg, and A. M. Thompson (1996), Ozone, hydroperoxides, oxides of nitrogen, and hydrocarbon budgets in the marine boundary layer over the South Atlantic, *J. Geophys. Res.*, *101*, 24,221–24,234, doi:10.1029/95JD03631.

Helmig, D., W. Pollock, J. Greenberg, and P. R. Zimmerman (1996), Gas chromatography mass spectrometry analysis of volatile organic trace gases at Mauna Loa Observatory, Hawaii, *J. Geophys. Res.*, *101*, 14,697–14,710, doi:10.1029/96JD00212.

Jöckel, P., et al. (2006), The atmospheric chemistry general circulation model ECHAM5/MESSy: 1. Consistent simulation of ozone from the surface to the mesosphere, *Atmos. Chem. Phys.*, *6*, 5067–5104.

Kawa, S. R., and R. Pearson Jr. (1989), Ozone budgets from the dynamics and chemistry of marine stratocumulus experiment, *J. Geophys. Res.*, *94*, 9809–9817, doi:10.1029/JD094iD07p09809.

Kettle, A. J., and M. O. Andreae (2000), Flux of dimethylsulfide from the oceans: A comparison of updated data sets and flux models, *J. Geophys. Res.*, *105*, 26,793–26,808, doi:10.1029/2000JD900252.

Kieber, R. J., L. H. Hydro, and P. J. Seaton (1997), Photo-oxidation of triglycerides and fatty acids in seawater: Implication toward the formation of marine humic substances, *Limnol. Oceanogr.*, *42*, 1454–1462.

Lelieveld, J., and F. J. Dentener (2000), What controls tropospheric ozone?, *J. Geophys. Res.*, *105*, 3531–3551, doi:10.1029/1999JD901011.

Lenschow, D. H., R. Pearson Jr., and B. B. Stankov (1982), Measurements of ozone vertical flux to ocean and forest, *J. Geophys. Res.*, *87*, 8833–8837, doi:10.1029/JC087iC11p08833.

Louanchi, F., and R. G. Najjar (2000), A global monthly climatology of phosphate, nitrate and silicate in the upper ocean: Spring-summer export production and shallow mineralization, *Global Biogeochem. Cycles*, *14*, 957–977, doi:10.1029/1999GB001215.

Magi, L., F. Schweitzer, C. Pallares, S. Cherif, P. Mirabel, and C. George (1997), Investigation of the uptake rate of ozone and methyl hydroperoxide by water surfaces, *J. Phys. Chem. A*, *101*, 4943–4949, doi:10.1021/jp970646m.

Matrai, P., M. Vernet, and P. Wassmann (2006), Relating temporal and spatial patterns of DMSP in the Barents Sea to phytoplankton biomass and productivity, *J. Mar. Syst.*, *63*, 83–101.

McKay, W. A., B. A. Stephens, and G. J. Dollard (1992), Laboratory measurements of ozone deposition to sea water and other saline solutions, *Atmos. Environ.*, *26A*, 3105–3110.

Oh, I.-B., D. W. Byun, H.-C. Kim, S. Kim, and B. Cameron (2008), Modeling the effect of iodide distribution on ozone deposition to seawater surface, *Atmos. Environ.*, *42*, 4453–4466.

Olivier, J. G. H., J. A. van Aardenne, F. Dentener, L. Ganzeveld, and J. A. H. W. Peters (2005), Recent trends in global greenhouse gas emissions: Regional trends and spatial distribution of sources, *Environ. Sci.*, *2*, 81–99, doi:10.1080/15693430500400345.

Pedersen, T., and K. Sehested (2001), Rate constants and activation energies for ozonolysis of isoprene, methacrolein andmethyl-vinyl-ketone in aqueous solution: Significance to the in-cloud ozonation of isoprene, *Int. J. Chem. Kinet.*, *33*, 182–190, doi:10.1002/1097-4601(200103)33:3<182::AID-KIN1012>3.0.CO;2-D.

Peltzer, E. T., and N. A. Hayward (1996), Spatial and temporal variability of total organic carbon along 140 degrees W in the equatorial Pacific Ocean in 1992, *Deep Sea Res., Part II*, *43*, 1155–1180, doi:10.1016/0967-0645(95)00014-3.

Rebello, A. L., F. W. Herms, and K. Wagener (1990), The cycling of iodine as iodate and iodide in a tropical estuarine system, *Mar. Chem.*, *29*, 77–93.

Riemer, D. D., P. J. Milne, R. G. Zika, and W. H. Pos (2000), Photoproduction of nonmethane hydrocarbons (NMHCs) in seawater, *Mar. Chem.*, *71*, 177–198, doi:10.1016/S0304-4203(00)00048-7.

Roeckner, E., et al. (2003), The atmospheric general circulation model ECHAM5. Part I: Model description, *Rep. 349*, Max-Planck Inst. for Meteorol., Hamburg, Germany. (Available at http://www.mpimet.mpg.de).

Saiz-Lopez, A., et al. (2008), On the vertical distribution of boundary layer halogens over coastal Antartica; implications for O_3, HO_x, NO_x, and the Hg lifetime, *Atmos. Chem. Phys.*, *8*, 887–900.

Sander, R. (1999), Modeling atmospheric chemistry: Interactions between gas-phase species and liquid cloud/aerosol particles, *Surv. Geophys.*, *20*, 1–31, doi:10.1023/A:1006501706704.

Sander, R., A. Kerkweg, P. Jöckel, and J. Lelieveld (2005), Technical note: The new comprehensive atmospheric chemistry module MECCA, *Atmos. Chem. Phys.*, *5*, 445–450, sRef-ID:1680–7324/acp/2005–5-445.

Schwartz, S. E. (1992), Factors governing dry deposition of gases to surface water, in *Precipitation Scavenging and Atmosphere-Surface Exchange, Coords.*, vol. 2, edited by S. Schwartz and W. G. N. Slinn, pp. 789–801, Hemisphere Publ., Washington, D. C.

Seinfeld, J. (1986), *Atmospheric Chemistry and Physics of Air Pollution*, Wiley-Intersci., Malden, Mass.

Shon, Z.-H., and N. Kim (2002), A modeling study of halogen chemistry's role in marine boundary layer ozone, *Atmos. Environ.*, *36*, 4289–4298, doi:10.1016/S1352-2310(02)00426-0.

Taylor, K. E., D. Williamson, and F. Zwiers (2000), The sea surface temperature and sea-ice concentration boundary conditions for AMIP II simulations, *PCMDI Rep. 60*, 25 pp., Program for Clim. Model Diagn. and Intercompar., Lawrence Livermore Natl. Lab., Livermore, Ca.

Tiefenau, H., and P. Fabian (1972), The specific ozone destruction at the ocean surface and its dependence on horizontal wind velocity from profile measurements, *Meteorol. Atmos. Phys.*, *21*, 399–412, doi:10.1007/BF02245584.

Tost, H., P. Jöckel, A. Kerkweg, R. Sander, and J. Lelieveld (2006), Technical note: A new comprehensive SCAVenging submodel for global atmospheric chemistry modelling, *Atmos. Chem. Phys.*, *6*, 565–574.

Truesdale, V. W., A. J. Bale, and E. M. S. Woodward (2000), The meridional distribution of dissolved iodine in near-surface waters of the Atlantic Ocean, *Prog. Oceanogr.*, *45*, 387–400, doi:10.1016/S0079-6611(00)00009-4.

Van Aardenne, J. A., F. Dentener, J. G. J. Olivier, J. A. H. W. Peters, and L. N. Ganzeveld (2005), The EDGAR 3.2 Fast Track 2000 dataset (32FT2000), Netherlands Environ. Assess. Agency, Bilthoven, Netherlands. (Available at http://www.mnp.nl/edgar/model/v32ft2000edgar/docv32ft2000/)

von Kuhlmann, R., M. G. Lawrence, P. J. Crutzen, and P. J. Rasch (2003), A model for studies of tropospheric ozone and nonmethane hydrocarbons: Model description and ozone results, *J. Geophys. Res.*, *108*(D9), 4294, doi:10.1029/2002JD002893.

Wesely, M. L., and B. B. Hicks (2000), A review of the current knowledge on dry deposition, *Atmos. Environ.*, *34*, 2261–2282, doi:10.1016/S1352-2310(99)00467-7.

Wesely, M. L., D. R. Cook, and R. M. Williams (1981), Field measurement of small ozone fluxes to snow, wet bare soil, and lake water, *Boundary Layer Meteorol.*, *20*, 459–471, doi:10.1007/BF00122295.

Yokouchi, Y., H. Mukai, K. Nakajima, and Y. Ambe (1990), Semi-volatile aldehydes as predominant organic gases in remote areas, *Atmos. Environ.*, *24*, 439–442.

C. W. Fairall, ESRL, NOAA, Boulder, CO 80305, USA.

L. Ganzeveld, Department of Environmental Sciences, Wageningen University and Research Centre, Wageningen, NL-6708 PB, Netherlands. (laurens.ganzeveld@wur.nl)

J. Hare, CIRES, University of Colorado, Boulder, CO 80309, USA.

D. Helmig, INSTAAR, University of Colorado, Boulder, CO 80309-0450, USA.

A. Pozzer, Energy, Environment and Water Research Center, Cyprus Institute, Nicosia, 1645, Cyprus.